



This is a repository copy of *Particle characterisation of rail sands for understanding tribological behaviour*.

White Rose Research Online URL for this paper:
<https://eprints.whiterose.ac.uk/185906/>

Version: Submitted Version

Proceedings Paper:

Skipper, W.A. orcid.org/0000-0001-8315-2656, Nadimi, S., Chalisey, A. et al. (1 more author) (Submitted: 2018) Particle characterisation of rail sands for understanding tribological behaviour. In: Li, Z. and Nunez, A., (eds.) Proceedings of the 11th International Conference on Contact Mechanics and Wear of Rail/Wheel Systems (CM 2018). 11th International Conference on Contact Mechanics and Wear of Rail/Wheel Systems (CM 2018), 24-27 Sep 2018, Delft, The Netherlands. TU Delft Library , pp. 886-895. ISBN 9789461869630

© 2018 The Author(s). This is an author-produced version of a paper submitted to the 11th International Conference on Contact Mechanics and Wear of Rail/Wheel Systems (CM 2018).

Reuse

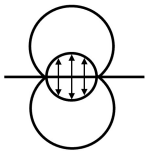
Items deposited in White Rose Research Online are protected by copyright, with all rights reserved unless indicated otherwise. They may be downloaded and/or printed for private study, or other acts as permitted by national copyright laws. The publisher or other rights holders may allow further reproduction and re-use of the full text version. This is indicated by the licence information on the White Rose Research Online record for the item.

Takedown

If you consider content in White Rose Research Online to be in breach of UK law, please notify us by emailing eprints@whiterose.ac.uk including the URL of the record and the reason for the withdrawal request.



eprints@whiterose.ac.uk
<https://eprints.whiterose.ac.uk/>



PARTICLE CHARACTERISATION OF RAIL SAND FOR UNDERSTANDING TRIBOLOGICAL BEHAVIOUR

W.A. Skipper^{1,*}, A. Chalisey², R. Lewis¹

¹ Centre for Doctoral Training in Integrated Tribology, The University of Sheffield, Sheffield, United Kingdom

² RSSB, The Helicon, One South Place, London, United Kingdom

* E-mail: waskipper1@sheffield.ac.uk

Abstract: Low adhesion between a train's wheel and the rail can cause performance and safety issues; in the rail industry this is mitigated by sanding. This paper outlines a particle characterisation framework and applies it to three types of silica sand. It was found that the size of the sand particles differed with sand type but all other measured characteristics were relatively similar. Tribological tests were then conducted under realistic contact pressures to study the sands' influence on traction under varying adhesion conditions. All sands increased traction in low adhesion contacts. Further work will investigate extending the range of particles.

Keywords: traction enhancement; sanding; particle characterisation; tribological testing; adhesion materials.

1. INTRODUCTION

Low adhesion between train wheels and the rail is estimated to cost the UK industry £345m per annum [1] with the majority of this cost coming during Autumn when weather conditions are sub-optimal. Low adhesion in the wheel/rail contact leads to costly delays [2] as well as safety issues due to the loss of traction when braking, potentially leading to SPADs (signals passed at danger) and in the worst case collisions [3]. Low adhesion becomes a major problem when the coefficient of traction between wheel and rail drops below 0.2 for acceleration and 0.09 for braking [2]. Low adhesion conditions can exist in the wheel/rail contact when a third body layer is present, such as: water [4], water and oxides [5], and leaves on the line which bond tightly to the rail [6].

As the cost of low adhesion is so high it is imperative that the rails should be cleaned of third body layers to increase adhesion within the contact, one of the methods for achieving this is sanding which has been in use for many years. Sanding is a train-borne system that activates whenever low adhesion is detected; the sand particles are discharged into the wheel/rail contact from a hopper via a hose directed at the contact in the opposite direction of the train's travel.

In a literature review [7] looking at the effect of sand characteristics on adhesion restoration it was found that previous research primarily focussed on the grain size of the sand [8]–[12]. Some research has also been conducted looking at the effect of particle hardness on restoring adhesion [13]. These studies suggested that larger particle sizes were more effective at restoring

traction/braking, but there did seem to be an upper limit at which larger particles were not being effectively entrained into the contact. There was also some evidence to suggest harder particles were more effective, but this relationship plateaued after the hardness went above that of quartz on the Mohs scale.

This paper aims to define a particle characterisation framework for sand particles and assess the effect of these particles in restoring traction using a small scale tribological test. This framework will allow future particle systems to be identified for possible use in future sanding applications.

Previous studies have largely ignored the particle's geometry, mineralogy, and physical properties all of which may have an effect on the adhesion recovery in the wheel/rail contact and on the particle's entrainment into said contact. This paper proposes a series of tests to assess these properties for different rail sands.

Application of sand can be studied by breaking up the sanding process into separate stages; the flow of the sand from the hopper and through the hose, the bounce of the particle when it first hits the wheel or rail, and the entrainment into the wheel/rail contact. The first two stages have been modelled as small scale tests and included in the characterisation framework.

Lastly, this paper uses a small scale test to assess the coefficient of traction of the rail sands in dry, wet and sycamore leaf extract contaminated conditions to assess their traction restoring capability.

2. METHODOLOGY

2.1. Particle Characterisation Methods

The particle characteristics were split into four groups; geometry, mineralogy, physical properties, and application. Within these groups characteristics were categorised and assigned a test method based on either a current standard or from adapting a test method used in literature. A summary of this is included in Table 1, and the methodologies will be detailed in the following section. For all tests a representative sample of sand was produced using a chute splitter (As outlined in ASTM C702 [14]) which reduces the maximum error due to variations in the sand particles to <5% [15].

Table 1 Characteristic with corresponding test method.

Particle Characteristic		Testing Method	Standard/Example Paper
Geometry	Size	Sieving/Image Analysis	BS 1377-2:1990 [16]/ ASTM E2651-13 [17]
	Shape	Image Analysis	ASTM E2651-13 [17]
Mineralogy		X-Ray Diffraction	Lafuente et al. [18]
Physical Properties	Density	Pycnometry	BS 1377-2:1990 [16]
	Hardness	Nanoindentation	Oliver & Pharr [19]
	Fracture Toughness	Microindentation	ASTM E2546-15 [20]
Application	Angle of Repose	Tilting Cylinder	Geldart et al. [21]
	Coefficient of Restitution	Recording of Bounce with High Speed Camera	Hastie [22]

2.1.1. Particle Geometry

2.1.1.1. Sieve Analysis

Sieving was carried out to assess particle size distribution as it is a simple, cost effective way of comparing different sand samples, the method used for sieving follows the method for sieving fine grained soils set out in BS1377-2:1990 [23]. The sieve apertures ranged from 2mm to 63µm. All the sieves were placed, in order from largest to smallest, onto a sieve shaker for 20 minutes to ensure the sand had been adequately sieved.

2.1.1.2. Image Analysis

The image analysis was carried out using the Morphologi G3S, an optical microscope with pre-programmed stage movements allowing multiple images to be taken of a large number of particles. The sand being tested was dispersed onto a sample plate using high pressures to separate particles and the image analysis machine scanned the area that particles were dispersed over. The captured images of the particles were subsequently binarized which allowed measurements to be taken of each individual particle. The circle equivalent diameter has been used in this study to characterise sand size. The circular equivalent diameter is the diameter of a circle with the same area as the measured particle.

In addition to particle size, particle shape measurements were taken from the image analysis as well. The measurements taken included:

- *Circularity*; the ratio between the perimeter of a circle of equivalent area to the particle and the actual perimeter of the particle. Circularity can take a value between 0-1 with 1 denoting a perfectly circular particle.
- *Convexity*; the ratio between the convex hull perimeter of the particle shape and its actual perimeter. The convex hull can be thought of as the shape an elastic band would take if put onto the 2D particle shape [24].

2.1.2. Mineralogy

X-ray diffraction (XRD) measurements of each sand were used to find the major constituent minerals for each sand. The measurements were carried out using a Siemens D5000 x-ray diffractometer and were scanned using Cu Kα1 radiation between slit angles of 5-80°. The data was then assessed using ICDD PDF-4+ 2018 software to identify and match characteristic peaks to elements in the software's database.

2.1.3. Physical Properties

2.1.3.1. Pycnometry

The density of each sand was measured using the small pycnometer method outlined in BS 1377-2:1990 [23]. A small change was made so that three specimens were measured at a time instead of just two, therefore giving more confidence in the validity of the results.

2.1.3.2. Indentation

Both nano and micro indentation was conducted on each specimen, partly to compare the methods' efficacies for measuring hardness on sand particles and also microindentation was needed to measure the fracture toughness of the particles.

The sand samples were prepared by cold mounting particles in an epoxy resin system and subsequently grinding a polishing the surface of the particles to achieve a suitable surface for indentation techniques.

Nanoindentation was carried out on a Hysitron TI Premier from Bruker using a Berkovich indenter and a 10,000 µN load. Nine indentations were performed on >5 particles for each specimen. The raw load vs displacement data was then analysed using the Oliver-Pharr method [19] to produce hardness results.

Microindentation was carried out on a Durascan -70 G5 from Struers using a HV0.3 loading conditions. The indentation was measured optically to produce a hardness value and the cracks at each corner were subsequently measured to find a value for fracture toughness from a formula derived by Antis et al. [25]:

$$K_C = \alpha \left(\frac{E}{H} \right)^{0.5} \left(\frac{P}{c^2} \right) \quad (1)$$

where K_C is fracture toughness, α is an empirical constant varying with tip indenter geometry ($\alpha = 0.032$ in this case), E is the Youngs modulus (obtained from the Oliver-Pharr nanoindentation method [19]), P is the load and c is the crack length. Daphalapurkar et al. [26] found this produced data that could be used to characterise sand at the granular level but is ineffective for bulk characterisation, something which is less of a problem in this case where the sand does not act as a bulk material when discharged from the sanding hose.

2.1.4. Application Characteristics

2.1.4.1. Angle of Repose Test

The angle of repose can be used as a quick and simple test for assessing the flowability of a powder system

[21], in this case the angle of repose was tested using a rotating cylinder method. The cylinder was rotated gradually until sliding occurs on the surface of the sand, after which the angle was measured, a diagram of this is included in Figure 1. The tests were run in dry conditions and with 0.2%wt and 3%wt moisture contents to assess the effect of moisture content on flowability, these values were chosen as they have been found to cause problems with sand flow in the hopper [13]. 400g of sand was dried for each test with the moisture being added afterwards by a pipette. Each test condition was run 5 times for each sand.

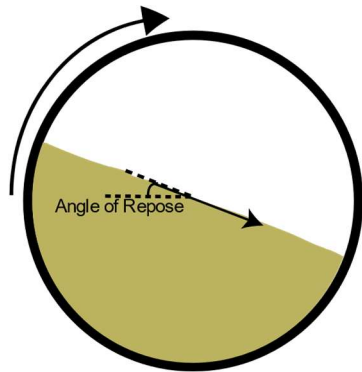


Figure 1 Revolving Cylinder Method Diagram.

2.1.4.2. Coefficient of Restitution Test

The coefficient of restitution was tested by carefully pushing a sand particle off of a platform and onto a rail with a high speed camera recording the particle bouncing on the rail; 20 particles from each sand were tested. A set of lights and white background were used to ensure sufficient contrast in order to clearly see the particle, a schematic of this set-up is included in Figure 2.

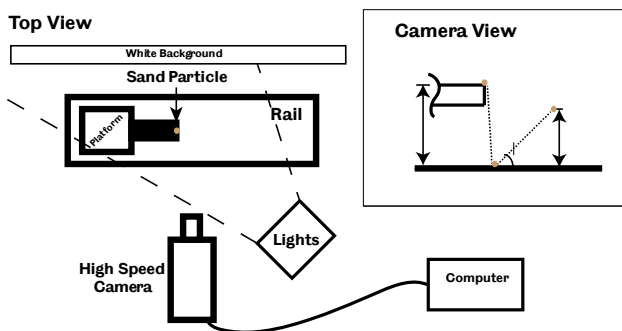


Figure 2 Coefficient of Restitution Test Set-up.

Taking the height of the platform as the particle's initial height and measuring the bounce height of the particle and the angle from where it bounced to its maximum bounce height, the coefficient of restitution (CoR) could be calculated:

$$CoR = \frac{\text{Velocity After Collision}}{\text{Velocity Before Collision}} \quad (2)$$

It has been found that particles that bounce lower tend to be more easily entrained into the wheel/rail contact [27], therefore identifying particles with lower CoR's, or even just characterising particle behaviour when

keeping low, may help improve understanding of how to improve entrainment.

2.2. Tribology Test Method

Pin-on-disc tests have been used in the past to study friction at high contact pressures (as seen in the wheel/rail contact), however due to the small contact area used in these tests granular materials are not appropriate to be studied as third body materials as a single particle may completely dominate the contact area, leading to unrealistic results. The high pressure torsion (HPT) rig is capable of achieving high contact pressures whilst also maintaining a large enough contact area for the particles not to dominate.

HPT rigs have been used as a workbench test of the wheel/rail contact with traction gels [28] and sand [29] as third body layers in the contact. These experimental methods were adapted for the testing conducted in this paper.

The HPT rig compresses a bottom specimen (made of R260 grade rail) together with a top specimen (made of R8T wheel) to create an annulus contact. A torque is applied to the bottom specimen until it has moved through a set sweep length at a low speed (<1 mm/s), a schematic of this action is included in Figure 3. Initially the surface deforms elastically until part of the surface plastically deforms and the contact enters slip.

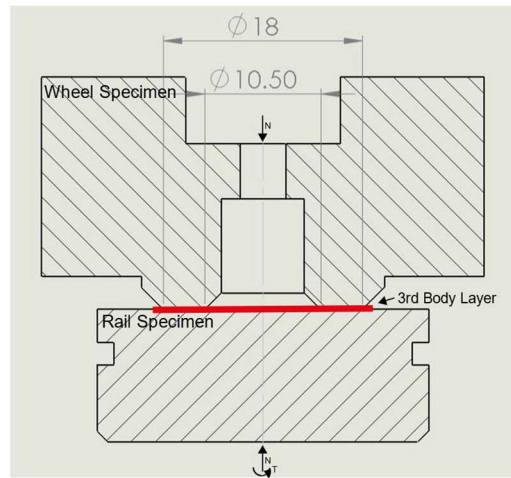


Figure 3 Schematic of HPT Interface.

The specimens were run together to fully shakedown the surfaces and the third body material was then added to the contact. For liquid contaminants 100 μ L was added using a pipette whilst 0.025g of sand was hand placed in sanded tests, an example of this sand placement has been included in Figure 4.



Figure 4 Sand Placement on HPT Sample.

Each sand type was tested in dry, wet, and leaf extract contaminated conditions for three runs. The annulus contact has an inner diameter of 10.5mm and an outer diameter of 18mm; a contact pressure of 900 MPa was used for all tests, with the maximum attainable torque being 1000 Nm.

2.3. Specimens

Three different sands have been studied in this paper:

- Garside 10/18 Sand; the current industry standard for sand used by the UK rail industry. Garside meets all the current UK sanding standards as set out in GMRT2461 [30].
- Central European (CE) Rail Sand; a representative sand currently being used in central European sanding operations.

- Youlgreave 110 Sand; currently sold commercially as an “anti-skid” sand. This sand was obtained from Derbyshire Aggregates.

3. RESULTS

3.1. Particle Characterisation

A summary of the particle characterisation results have been included in Table 2. This following section will describe the results included in this table in more detail.

In addition to the results listed in Table 2, images taken using an optical microscope have been included in Figure 5. These images are a representation of each sand which allows the reader to understand how the sands visually differ.

Table 2 Particle Characterisation Results.

Particle	Garside 10/18 Sand		Central European Rail Sand		Youlgreave 110 Sand	
Size (mm)	Sieve Analysis D ₅₀ : 1.30 Uniformity Coefficient: 1.34	Image Analysis Circle Equivalent Diameter D ₅₀ : 1.53	Sieve Analysis D ₅₀ : 0.92 Uniformity Coefficient: 1.49	Image Analysis Circle Equivalent Diameter D ₅₀ : 0.95	Sieve Analysis D ₅₀ : 0.55 Uniformity Coefficient: 1.56	Image Analysis Circle Equivalent Diameter D ₅₀ : 0.72
Shape	Circularity D ₅₀ : 0.88 Convexity D ₅₀ : 0.98		Circularity D ₅₀ : 0.84 Convexity D ₅₀ : 0.97		Circularity D ₅₀ : 0.84 Convexity D ₅₀ : 0.98	
Mineralogy	>90% Silica Titania & Calcium also present		Pure Silica		Pure Silica	
Density (g/cm ³)	2.65		2.64		2.67	
Hardness (GPa)	Nanoindentation: 12.0 ±2.2	Microindentation: 12.5 ±0.9	-	-	Nanoindentation: 12.1 ±2.8	Microindentation: 13.0 ±0.6
Fracture Toughness (MPa/m ^{0.5})	12.8 ±4.5		-		11.5 ±3	
Angle of Repose (°)	Dry: 32 3% Moisture Content: 45		Dry: 33 3% Moisture Content: 44		Dry: 32 3% Moisture Content: 65	
Coefficient of Restitution	0.49 ±0.14		0.44 ±0.16		0.49 ±0.20	

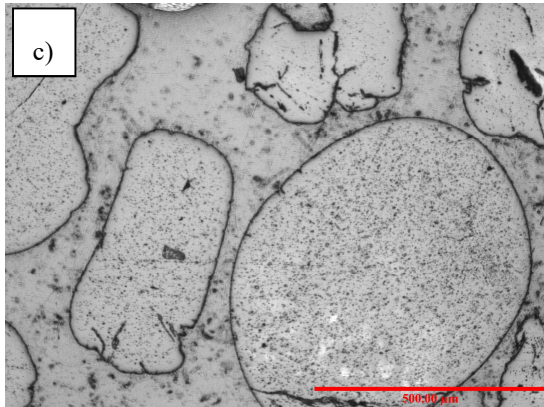
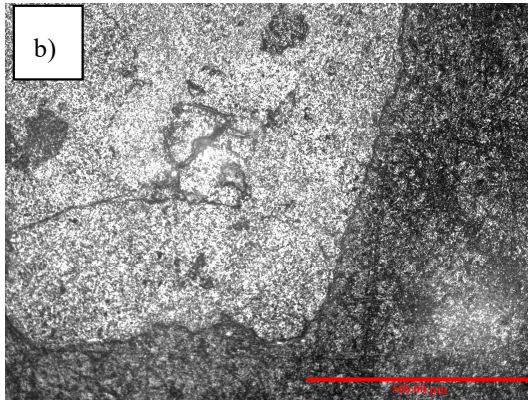
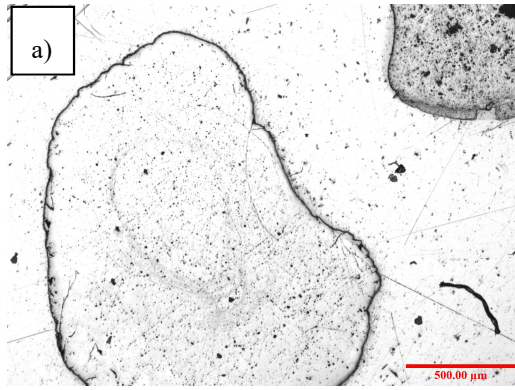


Figure 5 (a) Garside Particles; (b) CE Rail Particles ; (c) Youlgreave Particles.

3.1.1. Geometry

3.1.1.1. Sieve Analysis

The full sieve analysis has been included in Figure 6, where a cumulative volume graph shows the relative amount of sand passing through each sieve aperture. The median particle size (D_{50}) and the uniformity coefficient values were included in Table 2. Youlgreave sand was found to be the smallest sand as well as the least uniform, with Garside sand being the largest and most uniform.

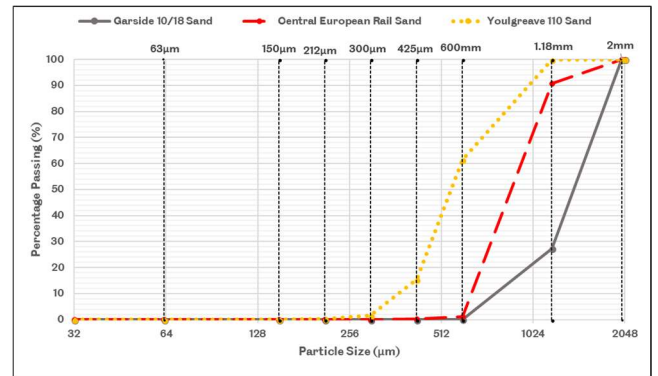


Figure 6 Cumulative Volumes from Sieve Analysis Data.

3.1.1.2. Image Analysis

As with the sieve analysis data, the data from the image analyses are presented as cumulative volume graphs with their median values included in Table 2. Circle equivalent diameter, circularity, and convexity have been plotted in Figure 7, Figure 8, and Figure 9 respectively. The Garside sand was the largest, with Youlgreave being the smallest sand. All sands were both relatively circular and non-convex though Garside sand was found to be very circular in comparison to the other two sands.

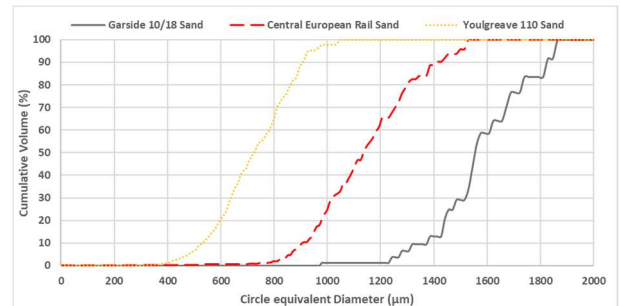


Figure 7 Circle Equivalent Cumulative Volumes.

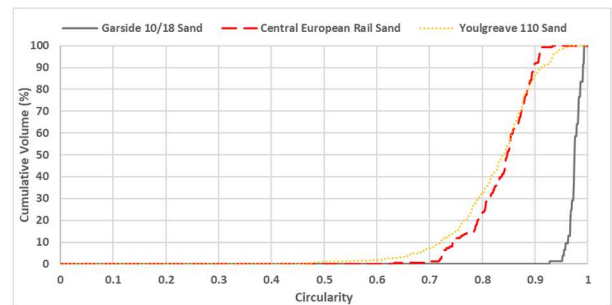


Figure 8 Circularity Cumulative Volumes.

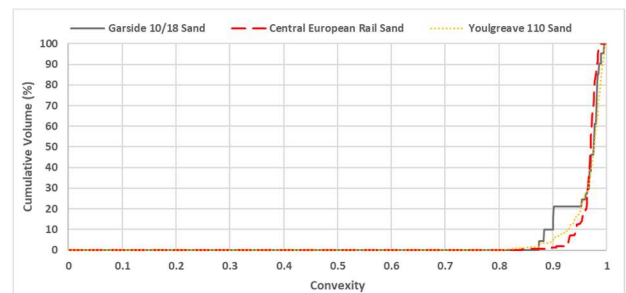


Figure 9 Convexity Cumulative Volumes.

3.1.2. Mineralogy

The mineral content for both the CE sand and the Youlgreave sand was found to be 100% silica. The Garside sand had ~5% titania content with <2% calcium also being present, the Garside sand was still >90% silica.

3.1.3. Physical

All the relevant data obtained from the physical tests has been included in Table 2. An example microindentation has been included in Figure 10, where the area of the indent was used to calculate hardness and the crack length was used to calculate fracture toughness.

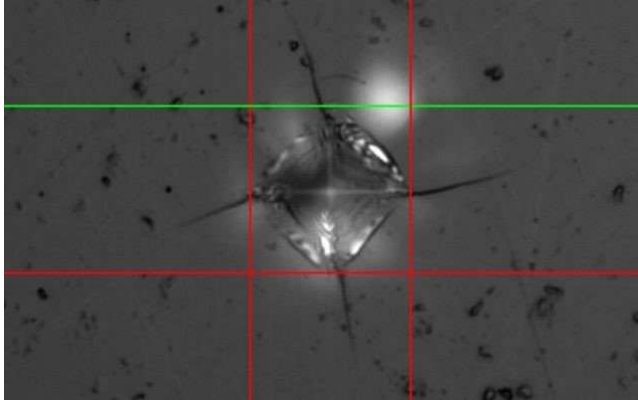


Figure 10 Example Measurement of Microindentation Hardness.

3.1.4. Application

3.1.4.1. Angle of Repose Test

There seemed to be very little effect on the angle of repose when 0.2% of moisture was added to all tested sands, this is readily apparent in Figure 11. At little to no moisture all the sands seem to have roughly the same angle of repose at 30-35°. However, when 3% moisture was added the angle of repose increased markedly for all sands. There was little difference between the Garside and the CE sand at 3%, with their angle of repose being ~45°, whereas the Youlgreave sand was affected by the moisture even more with a mean value of 65° being measured.

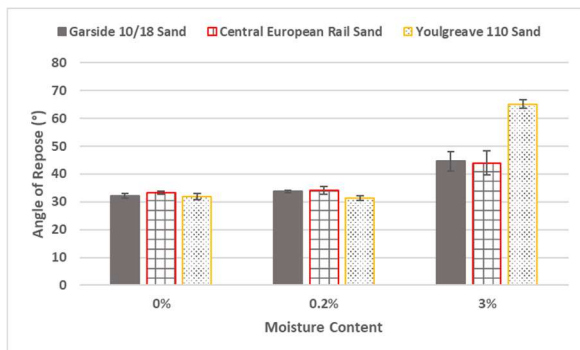


Figure 11 The Effect of Changing Moisture Content on Angle of Repose for all Rail Sands.

3.1.4.2. Coefficient of Restitution Test

The coefficient of restitution measurements have been summarised in Figure 12. Whilst the coefficients are all

roughly the same, between 0.44-0.49, the variance in results means a single value for each sand is a very unreliable way of comparing. The best way of analysing the data will be to characterise what different bounce behaviour is occurring between low and high coefficients.

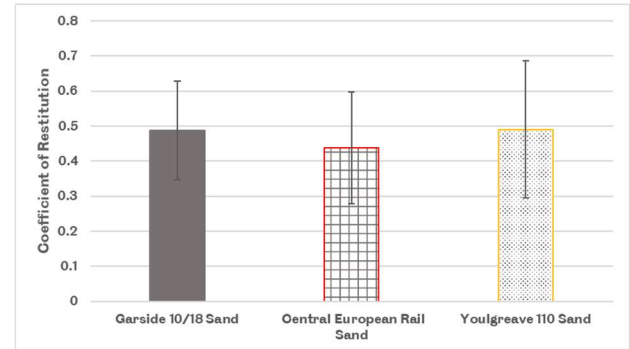


Figure 12 Coefficient of Restitution of All Sand Samples.

The best way to interpret the coefficient of restitution results is by characterising the different bounce behaviours of particles. From analysis of the videos it was observed that particles that kept low bounced sideways with a low angle relative to the rail, and had a lot of spin imparted onto them by the surface, whereas high bouncing particles showed little spin and went straight up, stills of these behaviours have been included in Figure 13. Similar results have been found in previous work on the CoR of irregular particles [22].

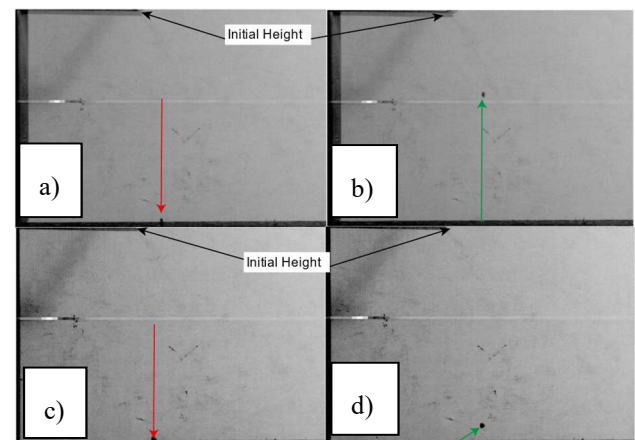


Figure 13 High CoR Behaviour: (a) Point of Contact, (b) Maximum Height Obtained; Low CoR Behaviour: (c) Point of Contact, (d) Maximum Height Obtained.

3.2. Tribological Testing

The contact conditions that produced the highest coefficient of traction were when the contact was dry, producing a coefficient of traction of ~0.8. When sand was added to a dry contact it lowered the coefficient of traction marginally to 0.7-0.8, with all the sands performing very similarly in both the stick and slip events. The change in coefficient of traction throughout the test sweep has been included in Figure 14.

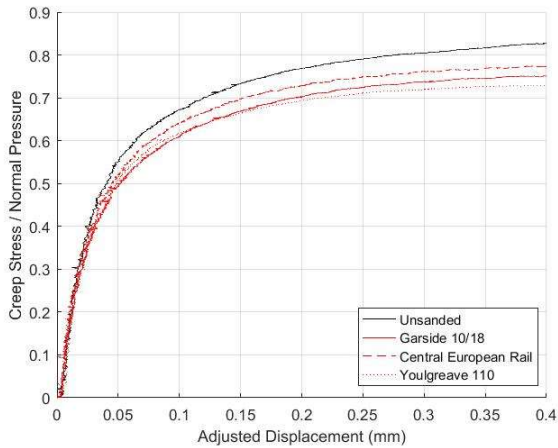


Figure 14 Effect of Sand on Dry HPT Interface.

When water was added to the contact the coefficient of traction dropped to just above 0.2 with a maximum coefficient of traction of 0.36 before the slip occurred, as can be seen in Figure 15. The Garside and CE sand both increased the coefficient of traction in the wet contact to above 0.5, though the Garside did this much more slowly than the CE sand which reached a maximum peak of just under 0.6, giving a similar curve shape to the wet unsanded contact. The Youlgreave sand was less effective, with the coefficient of traction only getting up to 0.4-0.5, as with the CE sand the coefficient of traction reached a peak before full sliding commenced.

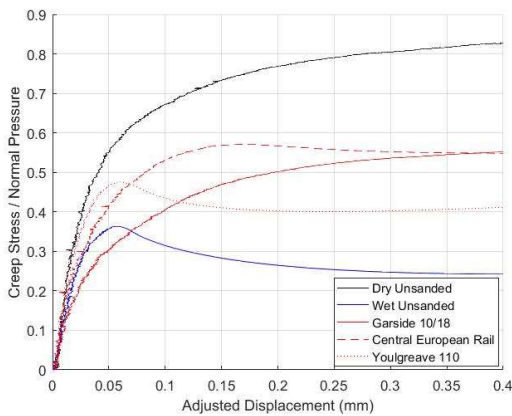


Figure 15 Effect of Sand on Wet HPT Interface.

The effect of the leaf extract on the contact was a lowered coefficient of traction, reducing to just above 0.2 thereby exhibiting the lowest tested coefficient of traction for all test conditions, this is apparent in Figure 16. Similar to the wet contact, peak traction was reached just before the onset of sliding. The Garside sand performed as it did in the wet test with traction being restored to above 0.5. The CE sand was less effective than it was in the wet contact, with the coefficient of traction peaking at just above 0.4. The Youlgreave sand was also less effective than in wet tests, only recovering traction to just above 0.3.

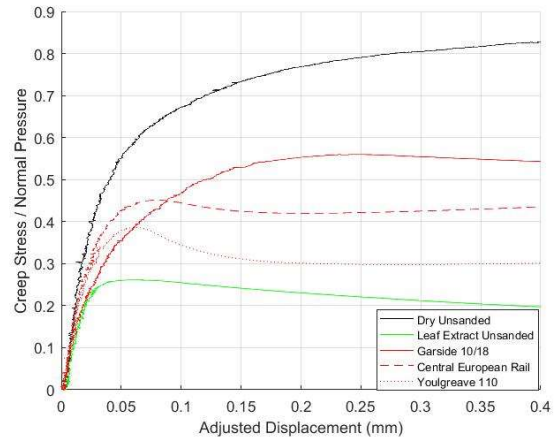


Figure 16 Effect of Sand on Leaf Contaminated Interface.

4. DISCUSSION

4.1. Comparing Sands

Both the Garside and CE sand were found to be of acceptable size according to the sand size criteria for braking (>90% sand between 0.71-2.8mm) as set out in the GMRT2461 sanding standards [30]; the Youlgreave sand was found to be smaller than currently acceptable. All tested sands were found to be fairly circular and non-convex which fits with the requirement for braking sand to be rounded and irregular.

The mechanical properties for Garside and Youlgreave sands were very similar perhaps unsurprising as they had similar mineral contents; mostly silica. The relatively large range of hardness, stiffness, and fracture toughness values was in large part due to the variation from one particle to the next; for Garside particles slightly differing mineralogy affected the particle structure which can be seen in Figure 5 where different particle types are evident. Both particles exhibited areas of hardness stratification with hardness values as low as 4-6 GPa in some areas, these are possibly due to small areas being affected by nearby pores lowering the measured hardness, evidence of the porous nature of both particles can also be seen in Figure 5. Microindentation was less affected by these small pores and therefore gave more consistent results. The German rail sand was found to be very porous (evidence of this can be seen in Figure 5), therefore the same indentation process could not be conducted upon it without improvements to the current preparation system.

With regards to the angle of repose tests, the dry values for all sands was found to be in line with literature findings [31]. All tested sands can be defined as free-flowing according to the Carr classification mentioned in a paper by Beakawi Al-Hashemi and Baghabra Al-Amoudi [32]. The large jump in the measured angle of repose when 3% moisture was added will be due to the water surface tension reducing flowability; this seemed to be especially pronounced for the Youlgreave sand, possibly due to its smaller size meaning it has a larger surface volume to mass ratio and therefore giving more sand surface for the water to stick upon.

4.2. Sieve Analysis vs Image Analysis

Whilst both image analysis and sieve analysis put the sands in the same order they both produced different values for sand size. This is due to the analyses measuring different dimensions and therefore not being directly comparable; image analysis measures the circle equivalent diameter, whereas the sieve analysis measures the second smallest dimension of a particle as the smallest aperture a 3D shape can fit through will be based on its smallest 2d projection which is dependent on its second smallest dimension.

The image analysis method used in this paper will generally overestimate the size of the sand; as the sand is lying on a 2D surface it will settle on its most stable base, generally its largest surface, leading to an image being taken of this surface. For more informative measurements future research should try to take a 3D image of the particle using x-ray tomography methods [33], [34].

4.3. Interpreting Coefficient of Restitution Results

The best way to interpret the coefficient of restitution results is by characterising the different bounce behaviours of particles. From analysis of the videos it was observed that particles that kept low bounced sideways with a low angle relative to the rail, and had a lot of spin imparted onto them by the surface, whereas high bouncing particles showed little spin and went straight up; these results are similar to previous work into the CoR of irregular particles [22]. The most likely cause for these different behaviours is due to the shape of a particle. In Figure 17 two particles are shown, the left particle's point of contact is directly below its centre of mass (CoM) thus the only forces acting on the sand (R) are straight up; the right particle has contacted the surface at a point away from its centre of mass creating a force couple which will cause the particle to spin and move sideways. A perfectly circular particle will always contact a flat surface at a point below its centre of mass, therefore the less circular a particle the higher chance of it bouncing low. To further examine this behaviour future work should measure the shape of individual particles and examine this effect on bounce behaviour.

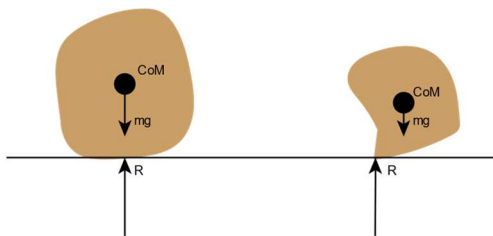


Figure 17 Diagram of Sand Bounce Behaviour.

4.4. Efficacy of Sands for Restoring Traction

The Garside rail sand was more than twice the size of the Youlgreave sand, bearing in mind larger particles have been shown to be more effective at restoring traction in a wheel/rail contact [8], [10] this may explain the Garside's better performance in HPT tests with the

CE sand being the second largest size sand and also the second best performer.

From visual inspections of the surface after testing it was apparent that not much was staying in the contact during the compression portion of the test, though there did seem to be more sand staying in the contact under wet conditions which was also an observation from a study by Lewis and Masing [35]. The sand that did stay in the contact was ground down to a fine powder by the large contact pressures in the interface.

None of the contact conditions went below the minimum coefficient of traction needed on UK railways (<0.2) [2], though the leaf extract contact came very close. Therefore, it is hard to say for certain whether all the tested sand would be effective in very low adhesion conditions. Future work will need to find a way of reducing friction further to truly test a sand's efficacy in low adhesion conditions.

5. CONCLUSIONS

Garside 10/18 sand was found to be the largest sand and the Youlgreave 110 sand was the smallest whilst the CE rail sand was in the middle, these results were the same for both sieve analysis and image analysis. The image analysis also found that all sands were fairly circular and non-convex with the Garside sand being very circular. According to previous work, the larger sand would be expected to give larger coefficients of traction in a tribological test, something which was found in the high pressure torsion tests in this paper.

Whilst all non-geometric characteristics were very similar for all types of sand, work will be undertaken characterising dissimilar particles as a part of future work. These particles characterised will include those used in current commercial traction enhancing products as well as particles used in industries other than rail for their anti-skid properties.

Three different baseline conditions were used for tribological testing: dry conditions, wet conditions, and sycamore leaf extract contaminated conditions. When sand was added to the baseline tests the contact produced coefficients of traction that are deemed acceptable on the UK rail network (>0.2) and showed significant increase in traction compared to wet and leaf extract conditions. Future testing should reduce the traction in baseline low friction tests to below 0.1 thereby testing the efficacy of sand in very low adhesion conditions.

The characterisation and tribological experiments performed in this paper outline a method for assessing future particles and investigating whether particles with particular characteristics are more effective at restoring traction in a wheel/rail contact. As well as characterising more particles, future work should focus on:

- The use of a particle's 3D shape when conducting image analysis.
- Investigate the relationship with particle shape and bounce behaviour.

- Conducting high pressure torsion tests under very low adhesion conditions.
- Assessing the impact of sand on wheel/rail surface wear and train detection.

Acknowledgements

The authors would like to thank the RSSB for part funding and guiding the work in this paper. In addition, the authors would like to thank the EPSRC for also part funding this research.

References

- [1] P. Gray, "T1107 Sander Trials Dissemination Event," 2018. [Online]. Available: <https://www.rssb.co.uk/Pages/adhesion.aspx>.
- [2] C. R. Fulford, "Review of low adhesion research (T354) (RSSB Report)," 2004. [Online]. Available: <https://www.sparkrail.org/Lists/Records/DispForm.aspx?ID=9539>.
- [3] Rail Accident Investigation Branch, "Autumn Adhesion Investigation Part 3: Review of adhesion-related incidents Autumn 2005 (RAIB Report)," 2007.
- [4] T. M. Beagley and C. Pritchard, "Wheel/rail adhesion - the overriding influence of water," *Wear*, vol. 35, no. 2, pp. 299–313, 1975.
- [5] L. Buckley-Johnstone, R. Lewis, K. Six, and G. Trummer, "Modelling and quantifying the influence of water on wheel / rail adhesion levels (RSSB Rport)," 2016. [Online]. Available: <https://www.sparkrail.org/Lists/Records/DispForm.aspx?ID=24280>.
- [6] K. Ishizaka, S. R. Lewis, and R. Lewis, "The low adhesion problem due to leaf contamination in the wheel/rail contact: Bonding and low adhesion mechanisms," *Wear*, vol. 378–379, pp. 183–197, 2017.
- [7] W. A. Skipper, A. Chalisey, and R. Lewis, "A Review of Railway Sanding System Research: Adhesion Restoration and Leaf Layer Removal," *Awaiting Publ.*, 2017.
- [8] O. Arias-Cuevas, Z. Li, R. Lewis, and E. a Gallardo-Hernández, "Laboratory investigation of some sanding parameters to improve the adhesion in leaf-contaminated wheel–rail contacts," *J. Rail Rapid Transit*, vol. 224, no. 3, pp. 139–157, 2010.
- [9] O. Arias-Cuevas and Z. Li, "Field investigations into the adhesion recovery in leaf-contaminated wheel–rail contacts with locomotive sanders," *J. Rail Rapid Transit*, vol. 225, no. 5, pp. 443–456, 2011.
- [10] O. Arias-Cuevas, Z. Li, and R. Lewis, "A laboratory investigation on the influence of the particle size and slip during sanding on the adhesion and wear in the wheel-rail contact," *Wear*, vol. 271, no. 1–2, pp. 14–24, 2010.
- [11] W. Wang, T. Liu, H. Wang, Q. Liu, M. Zhu, and X. Jin, "Influence of friction modifiers on improving adhesion and surface damage of wheel/rail under low adhesion conditions," *Tribology Int.*, vol. 75, pp. 16–23, 2014.
- [12] P. R. Cooper, "An investigation into the relationship between the Particle Size and the Frictional Performance of Sand (IM-ADH-011) (British Rail Report)," 1972. [Online]. Available: <https://www.sparkrail.org/Lists/Records/DispForm.aspx?ID=10483>.
- [13] F. G. R. Zobel, "Development of Remedies for Poor Adhesion (IM-ADH-019) (British Rail Research)," 1974. [Online]. Available: <https://www.sparkrail.org/Lists/Records/DispForm.aspx?ID=9038>.
- [14] ASTM, "ASTM C702-18: Standard Practice for Reducing Samples of Aggregate to Testing Size." 2018.
- [15] T. Allen, *Particle Size Measurement, 3rd Edition*. Chapman & Hall, 1981.
- [16] The British Standards Institution, "BS 1377-2:1990 Methods of test for Soils for civil engineering purposes — Part 2: Classification tests," *British Standard Institution*. 1990.
- [17] ASTM, "ASTM E2651-13: Standard Guide for Powder Particle Size Analysis." 2013.
- [18] B. Lafuente *et al.*, "Mineralogical characterization by XRD of gypsum dunes at White Sands National Monument and application to gypsum detection on Mars," in *45th Lunar and Planetary Science Conference*, 2014.
- [19] W. C. Oliver and G. M. Pharr, "An improved technique for determining hardness and elastic modulus using load and displacement sensing indentation experiments," *J. Mater. Res.*, vol. 7, no. 6, pp. 1564–1583, 1992.
- [20] ASTM, "ASTM E2546-15: Standard Practice for Instrumented Indentation Testing." 2015.
- [21] D. Geldart, E. C. Abdullah, A. Hassanpour, L. C. Nwoke, and I. Wouters, "Charcterization of Powder Flowability Using Measurement of Angle of Repose," *China Particuology*, vol. 4, no. 3–4, pp. 104–107, 2006.
- [22] D. B. Hastie, "Experimental measurement of the coefficient of restitution of irregular shaped particles impacting on horizontal surfaces," *Chem. Eng. Sci.*, vol. 101, pp. 828–836, 2013.
- [23] British Standards Institution, "BS 1377-2:1990 Methods of test for soils for civil engineering

- purposes. Part 2: Classification tests,” *British Standard*. 2010.
- [24] M. de Berg, O. Cheong, M. van Kreveld, and M. Overmars, *Computational Geometry: Algorithms and Applications, 3rd Edition*, 3rd ed. Springer-Verlag Berlin Heidelberg, 2008.
- [25] G. R. Anstis, P. Chantikul, B. R. Lawn, and D. B. Marshall, “A Critical Evaluation of Indentation Techniques for Measuring Fracture Toughness: I, Direct Crack Measurements,” *J. Am. Ceram. Soc.*, vol. 64, no. 9, pp. 533–538, 1981.
- [26] N. P. Daphalapurkar, F. Wang, B. Fu, H. Lu, and R. Komanduri, “Determination of Mechanical Properties of Sand Grains by Nanoindentation,” *Exp. Mech.*, vol. 51, no. 5, pp. 719–728, 2011.
- [27] S. R. Lewis, S. Riley, D. I. Fletcher, and R. Lewis, “Optimisation of a Railway Sanding System for Optimal Grain Entrainment into the Wheel/Rail Contact,” *J. Rail Rapid Transit*, 2016.
- [28] M. D. Evans, “Performance Assessment of Friction Management products in the Wheel-Rail Interface,” 2017.
- [29] D. I. A. Meierhofer, “A New Wheel-Rail Creep Force Model based on Elasto-Plastic Third Body Layers,” 2015.
- [30] Rail Safety and Standards Board, “GMRT2461 Sanding Equipment (Issue 2),” 2016. [Online]. Available: https://www.rssb.co.uk/rgs/standards/GMRT2461_Iss_2.pdf.
- [31] R. D. Holtz and W. D. Kovacs, *An Introduction to Geotechnical Engineering*. Prentice Hall, 1981.
- [32] H. M. Beakawi Al-Hashemi and O. S. Baghabra Al-Amoudi, “A review on the angle of repose of granular materials,” *Powder Technol.*, vol. 330, pp. 397–417, 2018.
- [33] D. Kong and J. Fonseca, “Quantification of the morphology of shelly carbonate sands using 3D images,” *Geotechnique*, vol. 68, no. 3, pp. 249–261, 2018.
- [34] T. Matsushima, J. Katagiri, K. Uesugi, A. Tsuchiyama, and T. Nakano, “3D Shape Characterization and Image-Based DEM Simulation of the Lunar Soil Simulant FJS-1,” *J. Aerosp. Eng.*, vol. 22, no. 3, pp. 15–23, 2009.
- [35] R. Lewis and J. Masing, “Static wheel / rail contact isolation due to track contamination,” *J. Rail Rapid Transit*, vol. 220, no. 1, pp. 43–53, 2006.